

## Photocatalytic Efficiency of Potassium Doped TiO<sub>2</sub> Nanowire-nanoparticle Hetero-structured Films Coated on Glass Substrate Under Visible Light Irradiation

Peerawas Kongsong <sup>a, \*</sup>, Phachcharee Phoempoon <sup>b</sup>, Mahamasuhaimi Masae <sup>c</sup>

<sup>a</sup> Department of Materials Engineering, Faculty of Engineering and Architecture, Rajamangala University of Technology Isan, Nakhon Ratchasima, 30000 Thailand

<sup>b</sup> Faculty of Industrial Technology, Songkhla Rajabhat University, Songkhla, 90000 Thailand

<sup>c</sup> Department of Industrial Engineering, Faculty of Engineering, Rajamangala University of Technology Srivijaya, Songkla, 90000 Thailand

Received 11 June 2018; Revised 27 August 2018; Accepted 27 August 2018

### Abstract

TiO<sub>2</sub> nanowire-nanoparticle hetero-structured films were prepared via sol-gel method, and coated on the glass substrates by the dipping method for the photocatalytic activity. The one-dimensional TiO<sub>2</sub> nanowires (NWs) were prepared by hydrothermal treatment with TiO<sub>2</sub> nanoparticles (NPs) commercially available. Different methods were used to characterize prepared nanowire-nanoparticle hetero-structured films including XRD, FESEM, XPS, and UV-Vis spectroscopy. The PWKT films were the highest photocatalytic activity on the degradation of methylene blue (MB). The PWKT films had about 4.5 fold degradation rate relative to undoped TiO<sub>2</sub>. Factors that affected the photoactivity of PWKT films were high crystallinity (NPs), small crystallite size (KT), narrow the energy band gap (WKT) and thickness of the films.

**KEYWORDS:** Hetero-structured films; Nanowire; Nanoparticle; K doped TiO<sub>2</sub>; Sol-gel method

\*Corresponding authors; e-mail: physics\_psu@windowslive.com

### Introduction

In materials science, recent progress is mainly devoted to developing innovative strategies to prepare nanomaterials with desired properties, which are a coupling of both its intrinsic and extrinsic properties. Among the strategies reported for extrinsic material properties control, nanoparticles agglomeration appears to be a promising approach to obtaining materials with controlled architectures and desired properties for targeted applications [1].

Titanium dioxide (TiO<sub>2</sub>) is one of the most popular oxide materials due to their superior characteristics in various applications including photoelectron chemistry. Titanium dioxide could display photocatalytic activities under UV light in 1972. A number of studies related to the photocatalytic performance of oxide semiconductor have been carried out. Being a star semiconductor photocatalyst, TiO<sub>2</sub> has many outstanding advantages, such as long term stability, non-toxicity, low cost, and environmentally benign nature [2]. Particularly, nanostructured TiO<sub>2</sub> have recently been of great interest because nanostructures often

improve photocatalytic performance and/or exhibit properties different from bulk counterparts [3]. In fact, combining a mixture of nanoparticles with different physical and chemical properties offers a large number of possibilities to tailor the properties of agglomerated materials. In addition to the properties of individual nanoparticles, their assembly gives rise to collective properties due to nanoparticles interaction. Compared with bulk material, this new configuration is more flexible for material preparation and extrinsic properties control [1]. However, the speed of electron diffusion across nanoparticles junctions is several orders of magnitude smaller than that of bulk crystalline TiO<sub>2</sub> due to frequent electron trapping at the junctions of nanoparticles. In this case, separated charges are recombined before they reach electrodes. One-dimensional TiO<sub>2</sub> nanostructures such as nanowires and nanotubes have been suggested to eliminate such problems. Nanowires can be grown from electrodes, providing a pathway of transporting charges without grain boundaries and junctions. Once electrons are injected to the conduction band of TiO<sub>2</sub>, recombination can be minimized due to their relatively wide

band gap. Another advantage of one-dimensional nanostructures is the ability to capture scattered light in the cell, which is possible to augment light harvesting. Nevertheless, the surface is required for dye absorption in one-dimensional structures not as large as that of porous nanoparticle films. In this regard, nanoparticle-nanowire hetero-structure may be able to maximize both dye absorption and charge transport. In addition, similar methodologies for enlarging surface areas of nanostructured metal oxides could be utilized for other applications including sensors and water splitting [3].

Many authors have reported that alkalis ( $x = \text{Na}, \text{K}, \text{Rb}$ ) [4, 5] doped titanium dioxide is attracting attention because of its potential as material for environmental photocatalysis. Although some authors claimed that the band gap of the solid is reduced due to a rigid valence band shift upon doping, others attribute the observed absorption of visible light by alkalis doped  $\text{TiO}_2$  to the excitation of electrons from localized impurity states in the band gap. Interestingly, it appears that the alkalis doping induced modifications of the electronic structure may be due to that the alkali ions penetrated into  $\text{TiO}_2$  lattice, or they probably are bonded with oxygen onto  $\text{TiO}_2$  surface to form alkalis oxides, both of the two factors restricted the growth of  $\text{TiO}_2$  nanocrystal [6].

The aim of this work was to assess the degradation of methylene blue solution by photocatalytic treatments, using  $\text{TiO}_2$  nanowire-nanoparticle hetero-structured films prepared via sol-gel method, and coated on a glass substrate by the dipping method for the photocatalytic activity. The nanowire powders (NWs) were synthesized by a hydrothermal method and mixed with  $\text{TiO}_2$  sol. The films were also characterized for their morphology, anatase crystallinity, and energy band gap and considered fundamental explanatory characteristics affecting photocatalytic activity.

## Materials and Methods

### *Preparation of K doped $\text{TiO}_2$ sol*

In the present study, the undoped  $\text{TiO}_2$  and K doped  $\text{TiO}_2$  (labeled as T and KT) were prepared by sol-gel method. In a typical preparation procedure, titanium (IV) isopropoxide (TTIP, 99.95%, Fluka Sigma-Aldrich) was added drop-wise under vigorous stirring to the mixture solution containing ethanol (99.9%; Merck Germany), 10 mL glacial acetic acid and potassium oxalate ((COOK)  $2\text{H}_2\text{O}$ ) was fixed at 3 mol% (From our previous study the potassium of 3 mol% was selected to dope into the  $\text{TiO}_2$  sol since it exhibits the higher photoactivity

compared to other concentrations) [6]. The mixture was stirred at room temperature at a speed of 800 rpm for 60 min to achieve the mole ratio of TTIP:  $\text{C}_2\text{H}_5\text{OH} = 1:82$  [7].

### *Preparation of NW powders*

Nanowire powders (NWs) were synthesized by a hydrothermal method. Commercially available Degussa P25 ( $\text{TiO}_2$  nanopowders purchased from Degussa Co, Germany ( $\text{TiO}_2$ , Degussa, Rutile: Anatase 85:15, 99.9%, 20 nm,  $50 \text{ m}^2 \text{ g}^{-1}$ )) were dissolved in 10 M NaOH solution [8]. In the preparation of NW powder, 1.000 g of the as-prepared  $\text{TiO}_2$  P25 nanoparticles mixed with 10 mL of  $10 \text{ mol L}^{-1}$  NaOH aqueous solution was added to the above mixture with a continuous sonication for 1 h, followed by hydrothermal post-treatment of the mixture in a 100 mL Teflon-lined autoclave at  $160 \text{ }^\circ\text{C}$  for 16 h. After this treatment, the obtained products were filtered, and then washed with  $0.1 \text{ mol L}^{-1}$   $\text{HNO}_3$  solution, distilled water and ethanol, respectively, followed by drying in an oven at  $80 \text{ }^\circ\text{C}$  for 4 h [9].

### *Preparation of $\text{TiO}_2$ nanowire-nanoparticle hetero-structured films*

$\text{TiO}_2$  nanowire-nanoparticle hetero-structured films were prepared via sol-gel method, and coated on glass substrates by the dipping method. A dip-coating apparatus was used to coat a glass substrate ( $2.54 \times 2.54 \times 0.30 \text{ cm}^3$ ). Before coating, substrates were cleaned consecutively by a high power sonic probe in distilled water, ethanol and acetone, and dried at  $80 \text{ }^\circ\text{C}$  for 15 min. First, 1.000 g of  $\text{TiO}_2$  P25 nanoparticles (NPs) and 1.000 g of NWs (labeled as PKT and WKT) were mixed with 50 mL of K doped  $\text{TiO}_2$  sol was added to the above mixture with a continuous sonication for 15 min. The  $\text{TiO}_2$  nanowire-nanoparticle hetero-structured films as-prepared by NWs were mixed with commercial  $\text{TiO}_2$  P25 NPs and were mixed with 50 mL of K doped  $\text{TiO}_2$  sol and added to the above mixture with a continuous sonication for 15 min. The mixing ratio of NPs and NWs were prepared with 50 wt% NWs and NPs in the mixture (labeled as PWKT). Then, the sol mixed was homogeneously coated on the substrates at the dipping speed of  $0.1 \text{ mm s}^{-1}$ . The coated substrates were dried at  $80 \text{ }^\circ\text{C}$  for 30 min and then heated at the temperature of  $400 \text{ }^\circ\text{C}$  for 1 h with a heating rate of  $10 \text{ }^\circ\text{C min}^{-1}$  [6].

### *Material Characterizations*

The surface morphology was investigated by field emission scanning electron microscopy (FESEM, JEOL, JSM). The chemical composition of sample surface was investigated by X-ray

photoelectron spectrometer (XPS; AXIS ULTRA<sup>DL</sup>, Kratos analytical, Manchester UK.) Spectrums were processed on software “VISION II” by Kratos analytical, Manchester UK. The base pressure in the XPS analysis chamber was about  $5 \times 10^{-9}$  torr. The samples were excited with X-ray hybrid mode  $700 \times 300 \mu\text{m}$  spot area with a monochromatic Al  $K_{\alpha 1,2}$  radiation at 1.4 keV. X-ray anode was run at 15 kV 10 mA 150 W. The photoelectrons were detected with a hemispherical analyzer positioned at an angle of  $45^\circ$  with respect to the normal to the sample surface. Crystallinity composition was characterized by using an X-ray diffractometer (XRD) (Phillips E’pert MPD, Cu-K $\alpha$ ). The crystallite size was determined from XRD peaks using the Scherer equation [10],

$$D = 0.9\lambda / \beta \cos\theta_{\beta} \quad (1)$$

where D is crystallite size,  $\lambda$  is the wavelength of X-ray radiation (Cu-K $\alpha = 0.15406$  nm),  $\beta$  is the angle width at half maximum height, and  $\theta_{\beta}$  is the half diffraction angle of the centroid of the peak in degrees. The band gap energies of TiO<sub>2</sub> and TiO<sub>2</sub> hetero-structured films, in film form, were measured by UV-Vis spectroscopy.

#### Photodegradation of MB

The photocatalytic activity of TiO<sub>2</sub>, K doped TiO<sub>2</sub> and TiO<sub>2</sub> hetero-structured films were tested by means of photodegradation of MB solution 5 mL having an initial concentration of  $1 \times 10^{-5}$  M as an indicator under the fluorescence light of 50 W. The distance between a testing substrate and a light source is 32 cm. The photocatalytic reaction test was done in a dark chamber under visible light irradiation at various times up to 4 h. The remaining concentration of MB was determined by UV-Vis spectroscopy.

## Results and Discussion

#### XRD of TiO<sub>2</sub> Thin Films

The XRD patterns of TiO<sub>2</sub>, K doped TiO<sub>2</sub>, and TiO<sub>2</sub> hetero-structured films, after calcination of the thin films at 400 °C for 1 h, are shown in Figure 1. Comparisons of the JCPDS 21-1272 anatase card of ASTM (American Society for Testing and Materials), and the JCPDS 21-1276 rutile ASTM card, suggest that the TiO<sub>2</sub>, K doped TiO<sub>2</sub>, and TiO<sub>2</sub> hetero-structured films have anatase crystallinity with no obvious differences

between them in the three types of thin films. The very broad diffraction peak at (1 0 1) plane ( $2\theta = 25.3^\circ$ ) was due to small crystallite size of TiO<sub>2</sub>. The crystallite sizes calculated from Scherrer’s equation are shown in Table 1. The KT film calcined at 400 °C had the smallest 13.1 nm crystallite size. This may be due to the penetration of K ions into TiO<sub>2</sub> lattice, or they probably are bonded with oxygen onto TiO<sub>2</sub> surface to form K oxides, both of the two factors restricted the growth of TiO<sub>2</sub> nanocrystal [6]. The crystallite size increased from this with further mixed NPs-NWs because of the large crystallites of P25 (Table 1).

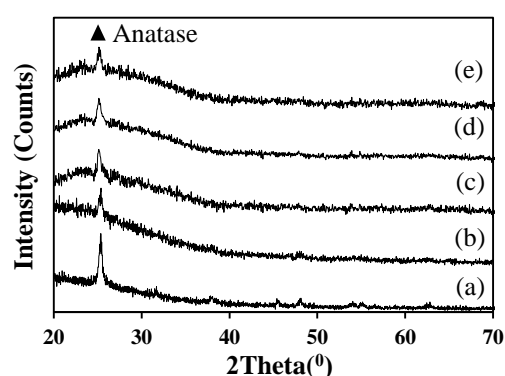
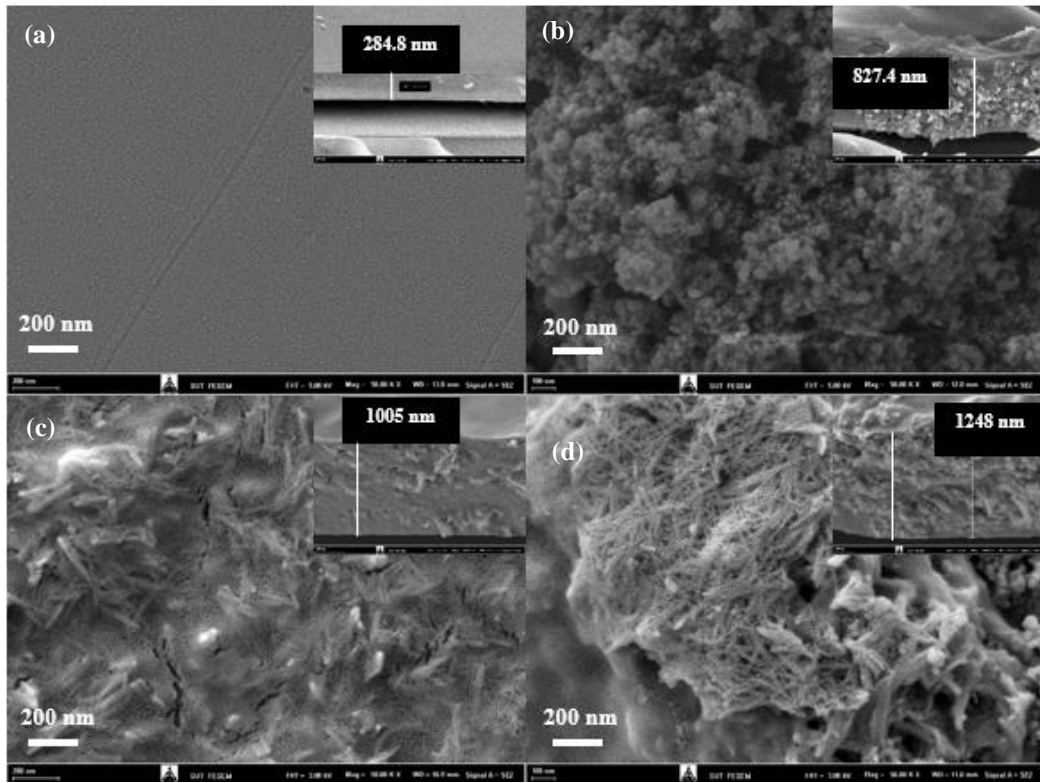


Fig. 1 XRD patterns of prepared films: (a) T, (b) TK, (c) PKT, (d) WKT, (e) PWKT.

#### Morphology of Thin Film Surface

The surface morphology of the coating on glass substrate was observed by FESEM as illustrated in Figure 2. It can be seen that the anatase crystallinity nucleated is homogeneous and the film surface was smooth in Figure 2a. FESEM micrograph of the PKT films exhibits nanoscale textures and is indicative of a much rougher surface in comparison with other samples (Figure 2b). FESEM results of PKT films also show that the P25 TiO<sub>2</sub> particles in the nanometer size range. From FESEM image of the as-made TiO<sub>2</sub> NWs (Figure 2c), it is clear that the TiO<sub>2</sub> NWs are abundant in quantity and pretty tidy with the smooth surface and have woven together, as can be seen from Figure 2d, a small and nanoparticles with the sizes of  $\sim 20$  nm were mixed with NWs on the surface of K doped TiO<sub>2</sub> prepared films. Figure 2a-2c (small figure) shows a cross-section of the TK, PKT, WKT and PWKT films of 285, 827, 1005 and 1248 nm thickness, respectively. NPs and NWs mixing displayed a significant effect on increases film in thickness.

smaller than that of pure TiO<sub>2</sub>. As a result, K



**Fig. 2** FESEM images of (a) TK, (b) PKT, (c) WKT and (d) PWKT films.

#### Energy gap determination

The UV-vis spectra of TiO<sub>2</sub>, K doped TiO<sub>2</sub> and TiO<sub>2</sub> hetero-structured films are shown in Figure 3. The absorption edge of the samples was determined by the following equation,

$$E_g = 1239.8/\lambda \quad (2)$$

where  $E_g$  is the band gap energy (eV) of the sample and  $\lambda$  (nm) is the wavelength of the onset of the spectrum. It is known that the band gap of TiO<sub>2</sub> can be calculated by extrapolation of the straight line from the absorption curve to the abscissa from UV-Vis absorbance spectra. The undoped TiO<sub>2</sub> (T) and K doped TiO<sub>2</sub> (KT) catalyst exhibited absorption only in the UV region with the absorption edge at about 343 and 344 nm, respectively. When K ions were incorporated into the lattice of TiO<sub>2</sub>, the growth of the particle size for as-prepared photocatalysts decreased and thus resulting in the broadening of the energy gap of TiO<sub>2</sub>. As listed in Table 1, the particle size of K doped TiO<sub>2</sub> samples was much

doped TiO<sub>2</sub> nanoparticle energy gap widened with the decrease of particle size and therefore led to a blue shift of optical absorption edge [11]. The band gap energy of WKT was shifted by 1.10 eV relative to 3.61 eV for pure TiO<sub>2</sub>. The band gap energy of WKT was 2.51 eV. The band gap energy of TiO<sub>2</sub> tend to decrease with mixing NW powders. The absorbance intensity decreased with increase in the thickness of the film surface.

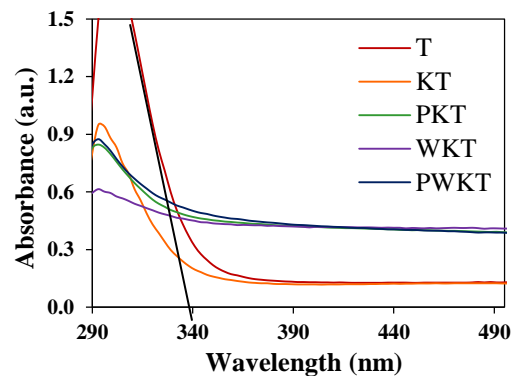


**Fig. 3** UV-Vis diffuse reflectance spectra of TK, PKT, WKT and PWKT films.

**Table 1** Crystallite sizes and energy band gaps of the calcined thin films prepared.

| Samples | Crystallite size (nm) | Energy band gap (eV) |
|---------|-----------------------|----------------------|
| T       | 29.7                  | 3.61                 |
| KT      | 13.1                  | 3.60                 |
| PKT     | 39.3                  | 3.17                 |
| WKT     | 17.2                  | 2.51                 |
| PWKT    | 22.1                  | 3.11                 |

*XPS analysis*

The electronic valence state of PWKT film was examined by XPS. The high-resolution XPS spectra of K 2p regions are shown in Figure 4. In addition to assessing the state of potassium atoms in the PWKT film, high-resolution XPS spectra of K 2p region were generated. The XPS spectra in K 2p region of PWKT film was deconvoluted and four peaks at 292.9 eV (K 2p3/2), 293.8 eV (K 2p3/2), 295.5 eV (K 2p1/2), and 296.4 eV (K 2p1/2) were obtained. In this work, the main peaks at binding energy of 292.9, 293.8 and 295.5 eV were attributed to the potassium atoms, whereas the peak at 296.4 eV was assigned to the potassium carbon [6]. The peaks at 292.9 eV (K 2p3/2) and 295.5 eV (K 2p1/2) were assigned to K-O groups [12].

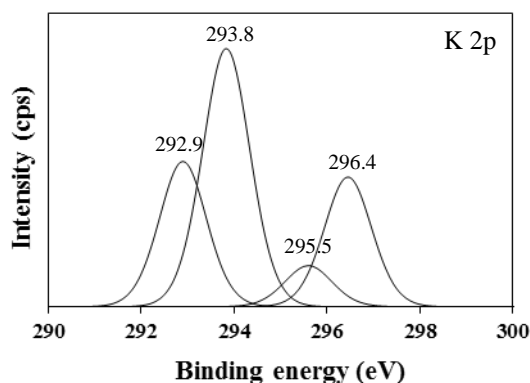


**Fig. 4** The high-resolution XPS spectra of K 2p on the surface of PWKT film.

*Photocatalytic Degradation of MB*

The photocatalytic activities of the films on glass substrates were determined for degradation of MB, with an initial concentration of  $10^{-5}$  M, under visible light for various irradiation times. The apparent degradation rate constant ( $k$ ) was chosen as the basic kinetic parameter to compare the photocatalysts, assuming the first order kinetics [13],

$$\ln(C_0/C) = kt \tag{3}$$

where  $C$  is the concentration of MB remaining in the solution at irradiation time  $t$ , and  $C_0$  is the initial concentration at  $t = 0$ . The observed  $\ln(C_0/C)$  vs. irradiation time is plotted in Figure 6, indicating that first order kinetics fit the data well. The fitted  $k$  values are in Table 2. The rate constant  $k$  was enhanced by doping, and the  $0.512 \text{ h}^{-1}$  rate constant for the PWKT film was about 4.5 folds relative to pure T film. The PWKT film had near optimal photoactivity across the range of compositions tested (Figure 6). According to prior reports, many factors affect the photoactivity of  $\text{TiO}_2$  photocatalysts, including crystallinity, grain size, specific surface area, surface morphology and surface state (surface OH radicals), and these factors are not independent but closely related to each other [14, 15]. Mixing NWs in KT film shifted light absorption wavelength to the visible region and narrowed the energy band gap to 2.51 eV. Well-crystallized anatase crystallinity facilitates the transfer of photo-induced vacancies from bulk to the surface for degradation of organic composites, and effectively inhibits the recombination between photo generated electrons and holes. The KT film had the smallest crystallite size, the WKT film had the narrowest the energy band gap, and the PKT film had high crystallinity. It was found that the photocatalytic activities of transparent prepared films increase with increasing the film thickness. The higher photocatalytic activities for the thicker  $\text{TiO}_2$  films originated from the greater amount of photogenerated electron and hole pairs, which were transferred from the inside to the surface of  $\text{TiO}_2$  films. The thicker film had the larger surface area because the surface roughness increased in general with the increase of film thickness. Thus, it is expected that the number of active sites on the  $\text{TiO}_2$  surface would increase [16]. Factors that affected the photoactivity of PWKT film were high crystallinity (NPs), small crystallite size (KT) and narrow the energy band gap (WKT).

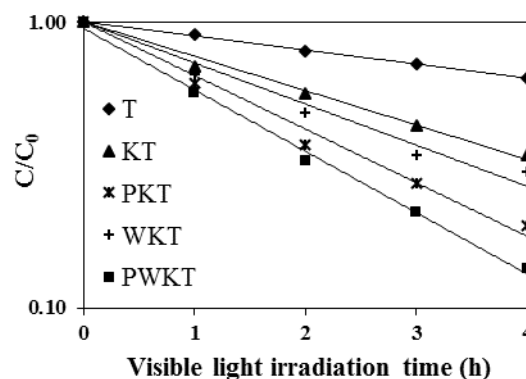


**Fig. 5** Photocatalytic degradation of MB by the prepared films coated on glass substrates are well approximated by first order kinetics.

**Table 2** The identified kinetics of photocatalytic degradation of MB

| Samples | Rate Equation         | Rate constant (k), h <sup>-1</sup> | R <sup>2</sup> |
|---------|-----------------------|------------------------------------|----------------|
| T       | $C/C_0 = e^{-0.113t}$ | 0.113 ± 0.001                      | 0.997          |
| KT      | $C/C_0 = e^{-0.277t}$ | 0.277 ± 0.004                      | 0.987          |
| PKT     | $C/C_0 = e^{-0.331t}$ | 0.331 ± 0.001                      | 0.966          |
| WKT     | $C/C_0 = e^{-0.423t}$ | 0.423 ± 0.003                      | 0.984          |
| PWKT    | $C/C_0 = e^{-0.512t}$ | 0.512 ± 0.002                      | 0.994          |

## Conclusion

TiO<sub>2</sub> nanowire-nanoparticle hetero-structured films were prepared via sol-gel method, and coated on the glass substrate by the dipping method. The prepared films were calcined at 400 °C for 1 h at a heating rate of 10 °C min<sup>-1</sup> in order to form crystalline anatase crystallinity of TiO<sub>2</sub>. K doping of TiO<sub>2</sub> films affected the crystallite size. The PWKT film was near optimal across the compositions tested, having the narrow band gap energy (NWs), high crystallinity of anatase crystallinity (NPs) and small crystallite size (K doped), and the highest photocatalytic activity on the degradation of MB. The PWKT film had about 4.5 fold degradation rate relative to undoped TiO<sub>2</sub>. The results suggest that PWKT film is advantageous for applications in sensors and water splitting.

## Acknowledgements

The authors would like to thank the Department of Materials Engineering, Faculty of Engineering and Architecture, Rajamangala University of Technology Isan for supporting this work. Dr. Mcwinner Yawman is also acknowledged for comments and suggestions, as he is the Research & Publication Expert and Trainer of the Institute of Research and Development Rajamangla University of Technology Isan.

## References

- [1] S. Mehrnaz, P. Kongsong, A. Taleb, N. Dokhane, L. Sikong, Large scale and facile synthesis of Sn doped TiO<sub>2</sub> aggregates using hydrothermal synthesis, *Sol. Energy Mater. Sol. Cells*. In press. 10(1) (2017) 1 – 9.
- [2] X. Zhang, Q. Liu, Preparation and characterization of titania photocatalyst co-doped with boron, nickel, and cerium. *Mater. Lett.* 6 (2008) 2589 – 2592.
- [3] C. Yu, J. Park, Thermal annealing synthesis of titanium-dioxide nanowire-nanoparticle hetero-structures. *J. Solid State Chem.* 183 (2010) 2268 – 2273.
- [4] Y. Bessekhoud, D. Robert, J.V. Weber, N. Chaoui, Effect of alkaline-doped TiO<sub>2</sub> on photocatalytic efficiency. *J. Photochem. Photobiol. A.* 167 (2004) 49 – 57.
- [5] P. Panagiotopoulou, D.I. Kondarides, Effects of alkali promotion of TiO<sub>2</sub> on the chemisorptive properties and water-gas shift activity of supported noble metal catalysts. *J. Catal.* 267 (2009) 57 – 66.
- [6] M. Masae, L. Sikong, P. Kongsong, C. Pholthawon, N. Pawanwatcharakorn, M.M.A.B. Abdullah, A.V. Sandu, Super hydrophilicity and photocatalytic activity of potassium doped TiO<sub>2</sub> nanoparticulate films, *Rev. Chim.* 67(9) (2016) 1884 – 1890.
- [7] P. Kongsong, L. Sikong, M. Masae, Photocatalytic degradation of 2, 4-dichlorophenol using N-doped SnO<sub>2</sub>/TiO<sub>2</sub> thin film coated glass fibers, *EnvironmentAsia*, 10(2) (2017)126 – 134.
- [8] H. Safajou, H. Khojasteh, M.S. Niasari, S.M. Derazkola, Enhanced photocatalytic degradation of dyes over graphene/Pd/TiO<sub>2</sub> nanocomposites: TiO<sub>2</sub> nanowires versus TiO<sub>2</sub> nanoparticles, *J. Colloid Interface Sci.* 498 (2017) 423 – 432.
- [9] W. Zhou, Y. He, Ho/TiO<sub>2</sub> nanowires heterogeneous catalyst with enhanced photocatalytic properties by hydrothermal synthesis method, *Chem. Eng. J.* 179 (2012) 412 – 416.

- [10] C. Liu, L. Zhang, R. Liu, Z. Gao, X. Yang, Z. Tu, F. Yang, Z. Ye, L. Cui, C. Xu, Y. Li, Hydrothermal synthesis of N-doped TiO<sub>2</sub> nanowires and N-doped graphene heterostructures with enhanced photocatalytic properties, *J. Alloys Compd.* 656 (2016) 24 – 32.
- [11] Z. Liuxue, L. Peng, S. Zhixing, Photocatalysis anatase thin film coated PAN fibers prepared at low temperature, *Mater. Chem. Phys.* 98 (2006) 111 – 115.
- [12] G. Yang, Z. Yan, T. Xiao, B. Yang, Low-temperature synthesis of alkalis doped TiO<sub>2</sub> photocatalysts and their photocatalytic performance for degradation of methyl orange, *J. Alloys Compd.* 580 (2013) 15 – 22.
- [13] T. Numpilai, T. Witoon, N. Chanlek, W. Limphirat, G. Bonura, M. Chareonpanicha, J. Limtrakul, Structure-activity relationships of Fe-Co/KAl<sub>2</sub>O<sub>3</sub> catalysts calcined at different temperatures for CO<sub>2</sub> hydrogenation to light olefins, *Appl. Catalysis A*, 547 (2017) 219 – 229.
- [14] P. Kongsong, L. Sikong, S. Niyomwas, V. Rachpech, Photocatalytic degradation of glyphosate in water by N-doped SnO<sub>2</sub>/TiO<sub>2</sub> thin-film-coated glass fibers, *Photochem. Photobiol.* 90 (2014) 1243 – 1250.
- [15] A.J. Zaleska, W. Sobezak, E. Grabowska, J. Hupka, Preparation and photocatalytic activity of boron modified TiO<sub>2</sub> under UV and visible light, *Appl. Catal. B.* 78 (2008) 92 – 100.
- [16] W.X. Xianyu, M.K. Park, W.I. Lee, Thickness effect in the photocatalytic activity of TiO<sub>2</sub> thin films derived from sol-gel process, *Korean J. Chem. Eng.* 18(6) (2001) 907 – 913.